Electrochemical behavior of indolone-*N*-oxides: Relationship to structure and antiplasmodial activity

Karine Reybier [a,b,*], Thi Hoang Yen Nguyen [a,b], Hany Ibrahim [a,b], Pierre Perio [a,b], Armelle Montrose [a,b], Paul-Louis Fabre [c,d,1], Françoise Nepveu [a,b]

[a] *Université de Toulouse, UPS, PHARMA-DEV, UMR 152, 118 route de Narbonne, F-31062 Toulouse cedex 9, France*
[b] *IRD, PHARMA-DEV, UMR 152, F-31062 Toulouse cedex 9, France*
[c] *Université de Toulouse, UPS, Laboratoire de Génie Chimique, F-31062 Toulouse cedex 9, France*
[d] *CNRS, Laboratoire de Génie Chimique, UMR 5503, F-31062 Toulouse cedex 9, France*

Keywords:
Indolone-*N*-oxides
Antimalarials
Cyclic voltammetry
EPR
Radical nitroxide anion

A B S T R A C T

Indolone-*N*-oxides exert high parasiticidal activity at the nanomolar level *in vitro* against *Plasmodium falciparum*, the parasite responsible for malaria. The bioreductive character of these molecules was investigated using cyclic voltammetry and EPR spectroelectrochemistry to examine the relationship between electrochemical behavior and antimalarial activity and to understand their mechanisms of action. For all the compounds (37 compounds) studied, the voltammograms recorded in acetonitrile showed a well-defined and reversible redox couple followed by a second complicated electron transfer. The first reduction ($-0.88\ V < E_{1/2} < -0.50\ V$ vs. SCE) was attributed to the reduction of the *N*-oxide function to form a radical nitroxide anion. The second reduction ($-1.65\ V < E_{1/2} < -1.14\ V$ vs. SCE) was assigned to the reduction of the ketone function. By coupling electrochemistry with EPR spectroscopy, the EPR spectra confirmed the formation of the nitroxide anion radical. Moreover, the experiments demonstrated that a slow protonation occurs at the carbon of the nitrone function and not at the NO function. A relationship between electrochemical behavior and indolone-*N*-oxide structure can be established for compounds with $R^1 = —OCH_3$, $R^2 = H$, and electron-withdrawing substituents on the phenyl group at R^3. The results help in the design of new molecules with more potent *in vivo* antimalarial activity.

1. Introduction

The *N*-oxide moiety is a reducible function that leads to biologically active compounds when introduced into conjugated systems such as heterocyclic and pseudo-quinoid compounds. These derivatives are thought to exert their biological action by the generation of reactive oxygen species through a redox cycling process that causes oxidative stress. This may explain how these compounds act as anti-infective agents towards a large number of microorganisms. This is the case of quinoxaline1,4-di-*N*-oxide derivatives acting as anti-infectious [1–4], or mono-*N*-oxides such as benzofuroxan, nitrofurane and nitroimidazole, derivatives with antiprotozoal activities [5–7], and of indolone-*N*-oxides with various antimicrobial activities [8–10]. The precise mechanism by which these drugs act in different biological models has not yet been fully elucidated [11]. Recently we reported the antimalarial activity of a series of indolone-*N*-oxides (Scheme 1). The biological evaluation and structure–activity relationship (SAR) studies proved the efficient antimalarial activity of these derivatives *in vitro* and *in vivo* against *Plasmodium falciparum* (*Pf*) [12,13]. Proteomic studies that we have reported suggest that these indolone-*N*-oxides cause a profound destabilization of the membrane of the *Pf* infected red blood cells (RBC) through a mechanism apparently triggered by the activation of a redox signaling pathway, which could be initiated by a chemical redox reaction in the RBC [14]. These results gave

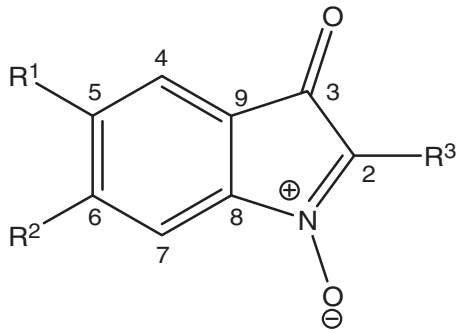

Scheme 1. Structure of the indolone-*N*-oxide series.

* Corresponding author at: PHARMA-DEV, UMR 152, Université Paul Sabatier, 118 route de Narbonne, F-31062 Toulouse cedex 9, France. Tel.: +33 562259804; fax: +33 562259802.
E-mail address: karine.reybier-vuattoux@univ-tlse3.fr (K. Reybier).
[1] The author is BES member.

doi:10.1016/j.bioelechem.2012.04.001

Table 1
Structure, cyclic voltammetric data, log P and antiplasmodial activity of indolone-*N*-oxide derivatives.

Compounds	R^1	R^2	R^3	$LogP^a_{calc}$ (VCCLAB)	IC_{50}/nM FcB1 strain[b]	$E_{1/2}/V$[d,e] (vs. SCE)	Rlp[f]	ΔEp/mV[g]
1	O—CH_2—O		4′-Chlorophenyl	2.07	75 ± 63	−0.705	0.27(1)	68
						−1.312	0.35	145
2	H	H	4′-Phenoxyphenyl	3.51	264 ± 60	−0.749	0.60(0.86)	77
						−1.510	0.10	275
4	H	H	4′-Methoxyphenyl	2.01	195 ± 20	−0.744	0.89(1)	68
						−1.264	0.48	113
5	H	H	4′-6′-Methoxy-naphthalen-2-yl	3.03	560 ± 15	−0.748	0.70(0.86)	71
						−1.425	0.17	116
7	O—CH_2—O		4′-Phenoxyphenyl	3.00	165 ± 40	−0.788	0.50(0.84)	80
						−1.405	0.46	198
8	H	H	3′, 4′-Dichlorophenyl	3.14	155 ± 20	−0.635	0.92(1)	66
						−1.370	0.28	98
9	OCH_3	H	4′-Chlorophenyl	2.58	210 ± 10	−0.727	1(1)	70
						−1.518	0.40	140
11	OCH_3	H	3′-Trifluoromethyl-4′-chlorophenyl	3.32	50 ± 39	−0.611	0.37(0.72)	75
						−1.317	0.50	182
12	H	OCH_3	4′-Chlorophenyl	2.57	148 ± 31	−0.729	0.85(0.95)	70
						−1.416	0.45	115
13	OCH_3	H	3′, 4′-Dichlorophenyl	3.18	100 ± 7	−0.634	0.89(1)	68
						−1.315	0.44	136
17	OCH_3	H	Phenyl	2.00	184 ± 53	−0.760	0.30(0.50)	100
						−1.518	0.15	148
18	OCH_3	H	4′-Tolyl	2.25	52 ± 48	−0.794	1(1)	74
						−1.588	0.35	176
19	H	CF_3	4′-Chlorophenyl	3.26	186 ± 15	−0.504	0.96(1)	76
						−1.276	0.55	149
20	OCH_3	H	4′-Methoxy-naphthalen-2-yl	3.03	135 ± 45	−0.620	0.37(?)	80
						−1.326	0.30	195
21	OCH_3	H	4′-Chlorobiphenyl-4-yl	4.06	630 ± 248	−0.726	1(1)	74
						−1.440	Irreversible	
22	OCH_3	H	4′-Methoxyphenyl	2.04	40 ± 39	−0.782	1(1)	72
						−1.650	0.44	166
24	OCH_3	H	4′-Phenoxyphenyl	3.51	193 ± 55	−0.750	0.96(1)	68
						−1.497	0.51	184
25	OCH_3	H	4′-Trifluoromethoxyphenyl	2.90	20 ± 0	−0.720	0.92(0.96)	68
						−1.590	0.85	172
26	OCH_3	H	4′-Dimethylaminophenyl	2.30	<3	−0.882	0.60(0.80)	82
						−1.570	Irreversible	
27	OCH_3	H	4′-Isopropoxyphenyl	2.81	17 ± 2	−0.816	0.89(1)	74
						−1.590	0.31	252
29	OCH_3	H	4′-Methoxy-3′-tolyl	2.25	44 ± 4	−0.836	0.75(1)	94
						−1.625	0.20	176
30	OCH_3	H	4′-Aminophenyl	1.58	24 ± 19	−0.876	0.83(1)	68
						−1.511	0.42	169
35	H	OCF_3	4′-Methoxyphenyl	2.88	133 ± 50	−0.681	0.95(1)	68
						−1.487	0.37	142
37	OCH_3	H	4′-Trifluoromethylphenyl	2.74	43 ± 23	−0.643	0.92(0.96)	68
						−1.387	0.45	200
39	OCH_3	H	3′-Chlorophenyl	2.60	21 ± 1	−0.698	0.92(1)	68
						−1.470	0.47	180
40	OCH_3	H	3′-Methyl-4′-tolyl	2.48	37 ± 28	−0.802	0.92(1)	74
						−1.574	0.44	226
42	OCH_3	H	4′-*Tert*-butylphenyl	3.63	204 ± 14	−0.791	1(1)	68
						−1.615	0.42	202
47	OCH_3	H	2′-Thiophen-3-yl	1.93	270 ± 16	−0.785	0.91(1)	70
						−1.573	0.34	232
48	H	NO_2	4′-Methoxyphenyl	1.97	345 ± 81	−0.477	0.81(1)	70
						−0.932	0.90	68
						−1.704	0.45	108
49	H	H	*i*-Butyl	1.61	>4,500[c]	−0.842	0.86(1)	64
						−1.549	0.60	192
50	H	H	*n*-Propyl	1.41	12,160 ± 500	−0.838	0.77(0.90)	80
						−1.457	0.41	194
56	H	H	4′-Nitrophenyl	1.96	56 ± 4	−0.518	0.90(1)	65
						−0.987	0.68	172
						−1.544	0.59	191
57	H	OPh	4′-Phenoxyphenyl	4.79	665 ± 135	−0.780	0.35(0.67)	74
						−1.425	0.40	138
60	H	H	4′-Ethylphenyl	2.81	2,750 ± 150	−0.726	0.67(1)	67
						−1.360	0.39	140
61	H	H	4′-Trifluoromethylphenyl	2.71	1,170 ± 80	−0.652	1(1)	72
						−1.434	0.36	132
67	H	$(CO)CH_3$	4′-Methoxyphenyl		584 ± 27	−0.603	0.79(1)	72
						−1.264	0.90	130
						−1.932	0.80	158

Table 1 (*continued*)

Compounds	R^1	R^2	R^3	$LogP^a_{calc}$ (VCCLAB)	IC_{50}/nM FcB1 strain[b]	$E_{1/2}/V$[d,e] (vs. SCE)	RIp[f]	ΔEp/mV[g]
68	OCH_3	H	4′-Dimethylamino-3′-tolyl		40 ± 30	−0.815 −1.612	0.66(1) 0.39	69 125

[a]LogP calculated with VCCLAB (http://www.virtuallaboratory.org/lab/alogps/start.html).
[b]The drug concentration giving a 50% decrease in parasite growth.
[c]The highest tested concentration.
[d]The electrochemical data are gathered at 0.1 V/s; for irreversible systems, $E_{1/2}$ was obtained under a higher potential scan rate when the backward peak appeared.
[e]$E_{1/2} = (Ep_{backward} + Ep_{forward})/2$.
[f]$RIp = |Ip_{backward}/Ip_{forward}|$; in parentheses, value when the potential scan is restricted to the first system.
[g]$\Delta Ep = |Ep_{backward} - Ep_{forward}|$.

rise to pharmacomodulation studies to develop new hits and leads. The conjugated system between the nitrone group and the ketonic function of the indolone moiety was found to be essential for optimal *in vitro* antiplasmodial activity.

In parallel, we explored some ADMET properties (Absorption, Distribution, Metabolism, Excretion and Toxicity) with the binding affinity of these compounds to human serum albumin [15] and cell based metabolism studies. In this context, we showed that indolone-*N*-oxides undergo a bioreductive transformation in red blood cells [16]. In previous studies we evaluated the spin trapping properties of these compounds and demonstrated their ability to trap hetero- and carbon-centered radicals [17]. Major differences in antiplasmodial activities as well as in spin trapping properties studied by EPR spectroscopy were observed between aryl and alkyl substituted indolones at R^3. It can be noted that indolone-*N*-oxides are built around three reducible functions, the *N*-oxide moiety, the highly electrophilic carbon in the nitrone moiety and the ketone function. At this point we considered it necessary to study the redox properties of indolone-*N*-oxides to establish the relationship between the electrochemical behavior and the biological activity and to continue with the study of the structures required to obtain more potent *in vivo* antimalarial activity.

We report here the redox behavior of 37 indolone-*N*-oxides using cyclic and stationary voltammetry, and EPR spectroelectrochemical measurements. The relationships between the substituents, redox potentials, lipophilicity and antiplasmodial activities were examined.

2. Experimental

2.1. Reagents

Acetonitrile (ACN, Fisher) and tetrabutylammonium perchlorate (TBAP, Fluka) were obtained commercially at the highest purity available and used without further purification. The methods for the synthesis of indolone-*N*-oxides have been previously reported [12]. The two new compounds (**67**, **68**) were obtained from Idealp-Pharma (Villeurbanne, France).

2.2. Voltammetric measurements

Electrochemical experiments were carried out at 25 °C in acetonitrile containing TBAP 0.1 mol L^{-1} using a Voltalab 80 PGZ 402 (Radiometer) with a conventional cell with three electrodes: reference electrode, a double junction calomel electrode (SCE); counter electrode, a platinum electrode sheet (5 × 5 mm); working electrode, a platinum disk (0.5 mm diameter) for cyclic voltammetry and a rotating disk electrode (EDI, Tacussel) for stationary conditions. All solutions were deoxygenated by argon bubbling through the solution for 15 min and maintaining a blanket of the inert gas over the solution during the experiment. Voltamperograms were recorded for a compound concentration equal to 10^{-3} mol L^{-1} (ferrocene or indolone-*N*-oxides) and a potential scan rate ranging from 0.02 V/s up to 25 V/s depending on experiments. The electrochemical data shown in Table 1 were recorded at a potential scan speed of 0.1 V/s.

2.3. EPR spectroelectrochemical analysis

For spectroelectrochemical measurements, the EPR spectrometer was coupled to a potentiostat-galvanostat (EG&G Princeton Applied Research-Model 362). A PHN 81 (Tacussel) voltammeter was used to control the applied potential. A flat quartz cell adapted to electrochemical measurements (Bruker, Wissembourg, France) was used for analysis. The electrochemical reduction was performed using a three-electrode set-up: the working and counter-electrode were platinum and the reference electrode was a silver wire. The applied potential was chosen to be on the diffusion plateau of the first reduction wave obtained under stationary conditions: $E_{applied} = E_{1/2} - 0.2$ V. The electrolysis potential was applied for 5 min to the solution containing the compound in acetonitrile/TBAP and the EPR spectrum was immediately recorded as a function of time. EPR spectra were obtained at X-band at room temperature on a Bruker EMX-8/2.7 (9.86 GHz) equipped with a high-sensitivity cavity (4119/HS 0205) and a gaussmeter (Bruker, Wissembourg, France). WINEPR and SIMFONIA software (Bruker, Wissembourg, France) were used for EPR data processing and spectrum computer simulation. Typical scanning parameters were scan rate, 1.2 G/s; scan number, 1; modulation amplitude, 1 G; modulation frequency, 100 kHz; microwave power, 20 mW; sweep width, 100 G; sweep time, 83.88 s; time constant, 40.96 ms; center field, 3 480 G; receiver gain 5×10^4.

2.4. Biological properties

Log P and antiplasmodial *in vitro* activities of the compounds studied have been previously reported [12] and are given in Table 1 (same numbering as in Ref. [12]). The IC_{50} value is defined as the concentration inhibiting the growth of the parasite *Pf* FcB1 reference strain by 50% when cultured in red blood cells.

3. Results and discussion

3.1. Electrochemical behavior

In the electroactivity domain of CH_3CN/TBAP, the cyclic voltammograms of the compounds showed oxidation and reduction processes at a platinum electrode. As this paper deals with the reductive properties of the indolone-*N*-oxides, only the cathodic behavior is described. Table 1 reports the electrochemical data obtained at a potential scan speed of 0.1 V/s: $E_{1/2} = (Ep_{backward} + Ep_{forward})/2$; $RIp = |Ip_{backward}/Ip_{forward}|$ and $\Delta Ep = |Ep_{backward} - Ep_{forward}|$.

Fig. 1 shows typical voltammograms obtained for the series. The voltammogram is characterized by two electron transfers. The first electron transfer (-0.882 (**26**) $< E_{1/2} < -0.477$ (**48**) vs. SCE) is perfectly reversible (RIp around 1) independently of the scan rate when the potential scan is restricted to this system. As expected the

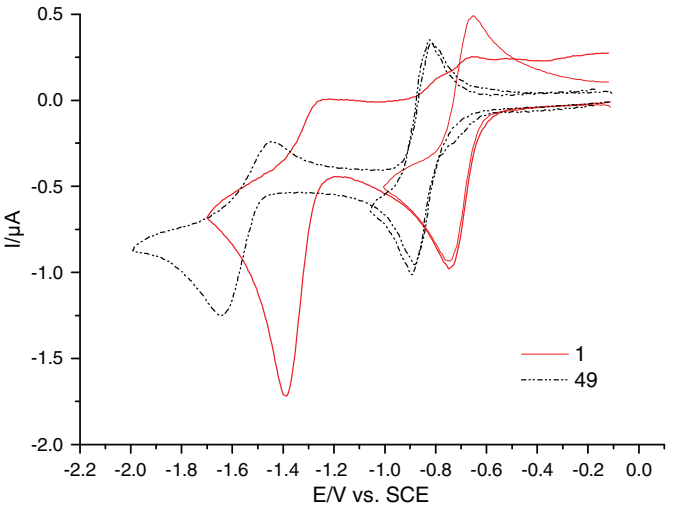

Fig. 1. Electrochemical properties of indolone-*N*-oxides. Cyclic voltammograms of **1** and **49** (1 mmol L^{-1}) at a platinum electrode in ACN-TBAP (0.1 mol L^{-1}), potential scan rate 0.1 V/s.

potentials $E_{1/2}$ depend on the nature of the substituents. The ΔEp values are in agreement with the quasi-reversible definition of an electron transfer. The peak currents are linearly related to the square root of the potential scan rate as for a diffusion controlled process. The second electron transfer (-1.704 (**48**)$<E_{1/2}<-1.264$ (**4, 67**) vs. SCE) is more complicated: the backward peak current is lower than the forward peak current (RIp<1). The peak currents are of the same order of magnitude as those of the first electron transfer, which means that the same number of electrons is exchanged. When the potential scan rate was increased, the electrochemical system became reversible; a simple EC scheme (electron transfer followed by a chemical reaction) could account for these observations. As above, the peak currents are linearly related to the square root of the potential scan rate as for a diffusion controlled process and the potentials $E_{1/2}$ depend on the nature of the substituents.

Considering the basic structure of the indolone-*N*-oxides (Scheme 1), two reducible functions are present, the *N*-oxide and the ketone, which may correspond to the two electron transfers observed by cyclic voltammetry. By contrast, compounds **48**, **56**, and **67**, that have a third reducible function in their structure such as NO_2 at R^2 (**48**), NO_2 at R^3 (**56**) and a ketone at R^2 (**67**), gave a third redox signal (Table 1).

By comparison with the oxidation peak current of ferrocene recorded under the same conditions, monoelectronic transfers are expected for the reductions of the indolone-*N*-oxide compounds. Moreover, as explained below, EPR spectroelectrochemical experiments demonstrated that the first reduction step gives rise to the appearance of a nitroxide radical-anion consistent with a monoelectronic transfer. These results confirm that the first reduction step can be attributed to the reduction of the *N*-oxide to a nitroxide radical-anion (Scheme 2). The second electron transfer is then attributed to the ketone function. The irreversibility of this reduction is indicative of high chemical reactivity of the intermediate, the radical-anion C•—O⁻.

The ketone reduction potential depends on the delocalization [18] whereas the nature of the products formed depends on the medium: pinacol, through a monoelectron transfer, or alcohol through a bielectron transfer [18,19] that requires protonation. Pinacol originates from the dimerization and then protonation of the radical-anion. The reversibility of the second electrochemical system depends on the stability of the radical-anion C•—O⁻: the peak ratio RIp is lower than unity (Table 1) but when the potential scan rate was increased (around 5 V/s) a quasi-reversible system was observed (data not shown). In dry acetonitrile, the one electron reduction yields the C•—O⁻ radical-anion, which gives pinacol after dimerization.

Voltammograms were recorded with increasing quantities of water (Fig. 2). Addition of small quantities of water has a slight effect on the first reduction process whereas it considerably affects the second one. The potential of the first redox process (*N*-oxide reduction) is slightly displaced towards less negative values when increasing the percentage of water (around 120 mV on the figure). Moreover, the system remains reversible, in particular when the potential scan is restricted to this system. The anodic displacement of the reduction potential can be explained by the protonation of the nitroxide radical-anion according to the potential-pH diagram theory, the water being the proton source. This protonation is confirmed by the EPR spectroelectrochemical analysis (cf. 3.2).

On the contrary, the potential of the second electron transfer (ketone reduction) is strongly displaced towards less negative values when the percentage of water is increased (around 500 mV). The forward peak current also increases showing that the system moves from a one electron transfer to a bielectronic transfer, leading to the production of alcohol [19,20].

For compounds **48**, **56**, and **67** that have a third reducible function in their structure, the signals are consistent with those reported in the literature. The acetophenone moiety in **67** is reduced around −2 V [20–22]. In the case of the NO_2 derivatives, their reductions are monoelectronic [23,24] in aprotic solvents. The potential of NO_2 reduction for **48** is then attributed at −0.932 V and for **56** at −0.987 V. The C=O reduction potentials are in the same order as the reported values of other compounds (Table 1). However, as part of our study, only the data corresponding to the first reduction step were correlated with anti-malarial properties.

3.2. EPR spectroelectrochemical analysis

To confirm the radical nature of the species formed after the first one-electron step reduction and to study its stability, electrochemistry was coupled with electron paramagnetic resonance (EPR) spectroscopy. An illustration of the EPR spectrum obtained and its evolution with time is shown in Fig. 3 for compound **1** after 5 min of electrolysis in acetonitrile containing TBAP 0.1 mol L^{-1} (potential on the plateau of the diffusion wave due to the first electrochemical system: $E_{applied}=E_{1/2}-0.2$ V). The spectrum recorded 4 min after the end of electrolysis (Fig. 3a) consists in a triplet characterized, as demonstrated by simulation, by the hyperfine splitting constants

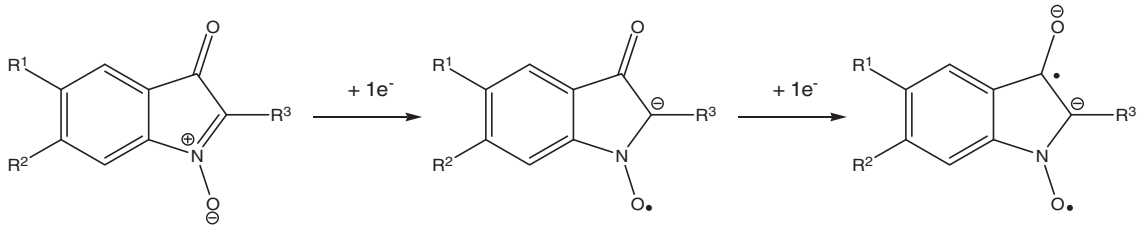

Scheme 2. Reduction of indole *N*-oxide.

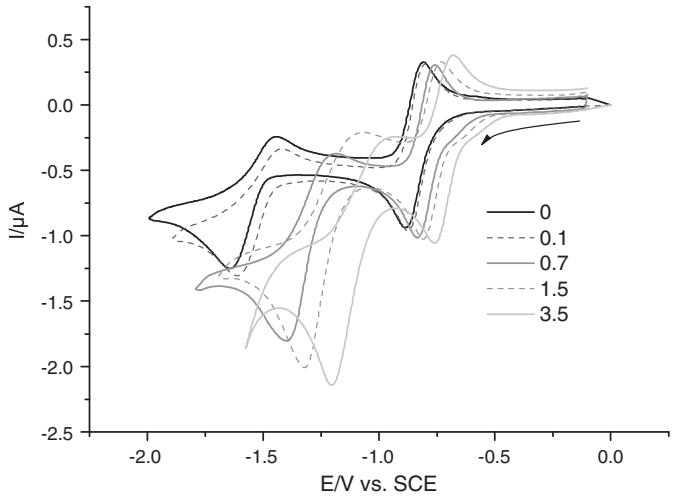

Fig. 2. Electrochemical properties of indolone-*N*-oxides. Cyclic voltammograms of **49** (1 mmol L^{-1}) at a platinum electrode in ACN-TBAP (0.1 mol L^{-1}) with increasing amount of water, potential scan rate 0.1 V/s.

$a_N = 6.27$ G, $a_H^{\gamma} = 1$ G (protons on carbons 4 and 7 for compound 1). This nitroxide radical-anion detected is relatively stable (about 10 min). This stability is consistent with an aprotic medium and the highly conjugated character of the indolone-*N*-oxide structure allowing the delocalization of the unpaired electron. The high stability of the spin adducts derived from indolone-*N*-oxides has already been demonstrated in previous studies dealing with spin trapping properties of these molecules [17]. This triplet evolves with time to a signal (Fig. 3c) with hyperfine splitting constants $a_N = 9.5$ G and $a_H^{\beta} = 2.3$ G indicating that the carbon of the nitroxide anionic form has been protonated (Scheme 3). A protonation on the nitroxide function would give a hydroxylamine form which is EPR silent. Before the protonation at carbon 2, the unpaired electron is strongly delocalized on the whole structure which is nearly planar and it couples with the nuclear spins of the nitrogen and proton at C4 and C7 (for compound 1). X-ray crystallography of a similar compound (2-phenylisatogen) shows that the isatogen ring and the phenyl ring are almost fully co-planar [25,26]. After protonation at C2, the planarity of the molecule is decreased thus reducing the electronic delocalization and resulting in a higher electronic density at the NO bond. The unpaired electron then couples with the nuclear spins of the nitrogen and

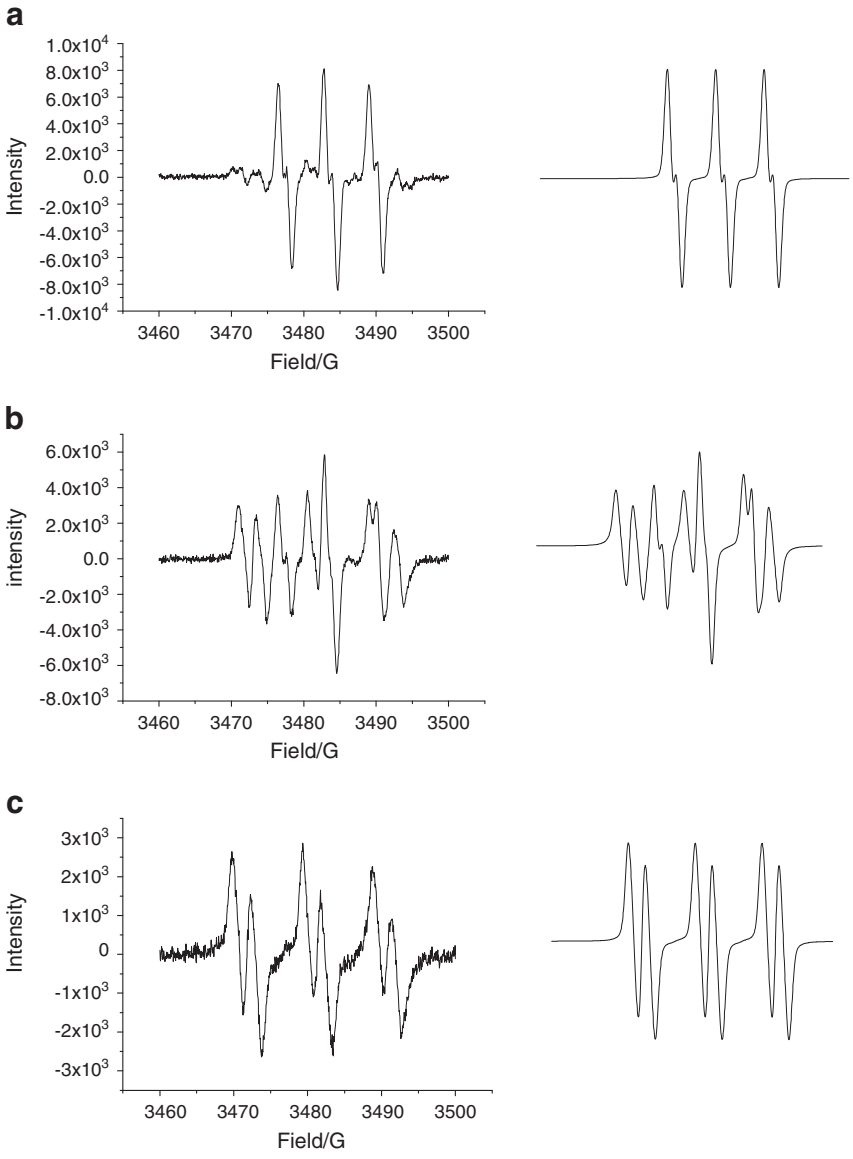

Fig. 3. EPR spectra of the reduced form of indolone-*N*-oxide: EPR spectra and the corresponding simulated spectra recorded for compound **1** (1 mmol L^{-1}) a) 4 min, b) 12 min and c) 23 min after the end of the 5 min electrolysis at −0.9 V vs. SCE in ACN containing TBAP (0.1 mol L^{-1}).

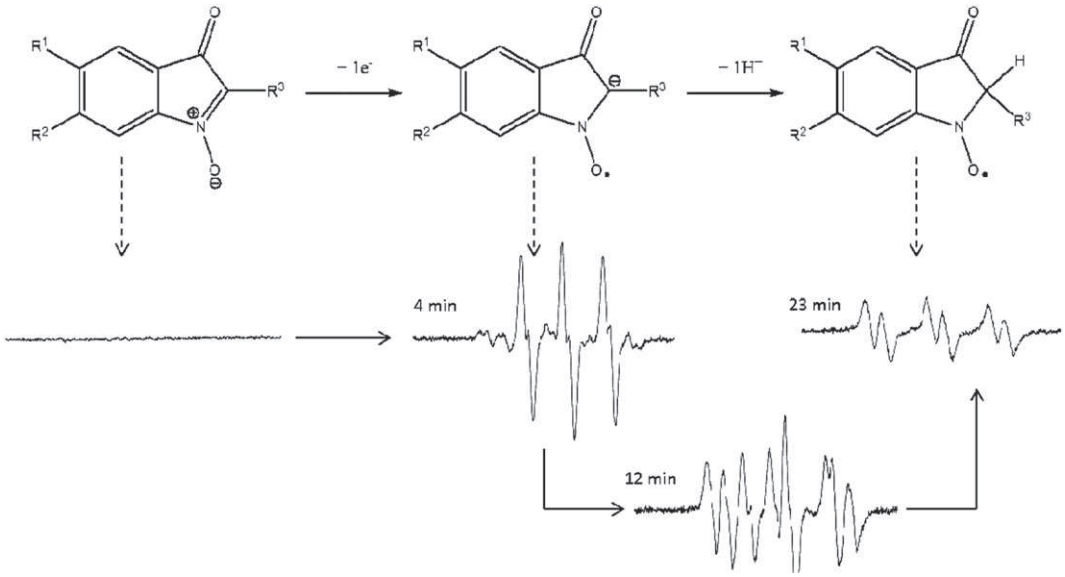

Scheme 3. Relationship between the reduced forms of indolone-*N*-oxides and the corresponding EPR spectra.

proton at C2. From this structural change resulting from the protonation at C2, the higher electronic density on the NO bond leads to a higher hyperfine splitting constant, a_N, shifting from 6.27 G to 9.5 G. These observations are in agreement with Scheme 3. For compound **1** a mixture of the two species (nitroxide radical-anion and its protonated form) is observed over about 8 min. As demonstrated by the simulation, the spectrum recorded 12 min after the end of electrolysis is the superimposition, in the same proportion, of the spectra of the two species (Fig. 3b). The coupling between the electrochemistry and EPR spectroscopy leads to a better understanding of each step of the reduction/protonation process compared with that reported for some isatogens [27].

3.3. Relationship between reduction potentials and substituents on indolone-N-oxides

All the compounds studied gave at least two electrochemical systems: the first one presented a half-wave potential ranging from −0.882 to −0.477 V vs. SCE while for the second one the limits are in the domain [−1.650, −1.264] V vs. SCE. These values are highly dependent on the three substituents, R^1, R^2 and R^3. Studies reported for other *N*-oxide derivatives, such as phosphorylated nitrones [28], phenyl-butyl nitrone derivatives [29] or quinoxaline-*N*, *N*′-dioxides [11], showed such a relationship. In our series, the presence of electron-donating groups induces an important shift of the first reduction wave. For example compounds **49** or **50**, (R^3 = alkyl) have the highest reduction potential value. With the introduction of electron-withdrawing substituents (Cl, CF_3, O—CF_3, NO_2) on the phenyl ring (R^3 = aryl) (compounds **1**, **8**, **9**, **11**, **12**, **13**, **19**, **25**, **37**, **39**, **56** and **61**) or on the indolone moiety at R^2 (compounds **19**, **35**, **48**), the products are more readily reduced. For example, the substitution of the alkyl chain (R^3) (compound **49** or **50**) by a 3,4-dichlorophenyl (compound **8**) or by a 4-trifluoromethylphenyl (compound **61**) group resulted in a positive shift equal to 23 mV for the first cathodic wave. This shift was only 9 mV when R^3 was a 4-ethylphenyl group (compound **60**). By comparing the redox potentials of compounds **9**, **37** and **25** or **56** and **61** the withdrawing effect of substituents appears clear: $NO_2 > CF_3 > Cl$. Similarly, by comparing compounds **37** and **25**, one can note that the replacement of CF_3 by O-CF_3 induces, as expected, a negative shift in the reduction potential. A smaller shift is recorded with the introduction of an electron-donating group (—O—R or —Ph—O—R) as R^1 or R^3 (compounds **2**, **4**, **5**, **7**, **18**, **20**, **22**, **24**, **27 29** and **57**). By comparing compounds **9** and **12** it appears that the position of the methoxy group (R^1 or R^2) did not affect the reduction potential.

These effects are consistent with the facilitation of reduction by lowering the electron density at C2 which is confirmed by the Hammett plot (Fig. 4), considering the σ_p values for substituents in the 4-position of the phenyl ring [27,30]. As predicted by Hammett, the number and position of electron-withdrawing groups influence the reduction potential.

Note that the most cathodic potentials were obtained in the case of amine substituents (compounds **26** and **30**). The addition of a

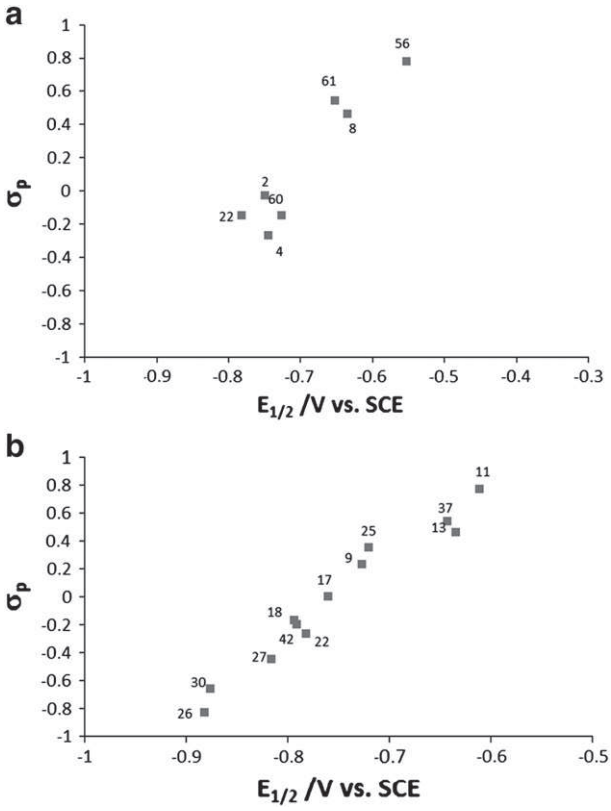

Fig. 4. Relationship between reduction potentials and Hammet constants of indolone-*N*-oxides. Plot of $E_{1/2}$ against Hammet substituent constants σ_p for compounds having (a) or not (b) OMe at R^3 [31].

methoxy group at R^1 does not modify the reduction potential as seen by comparing compounds **2** with **24** and **37** with **61**.

3.4. Relationship between the electrochemical behavior and antiplasmodial activity

The indolone-*N*-oxides gave rise to two reduction steps in ACN/TBAP. The first reduction of the *N*-oxide moiety is reversible and involves the formation of a stable nitroxide radical-anion as confirmed by EPR spectroscopy. This relatively stable radical could be the starting point for the redox events deleterious to the parasite. In this case, the ease of the first reduction of the *N*-oxide moiety would play an important role in the antiplasmodial activity. Indeed, further experiments carried out on the series have demonstrated that the antiplasmodial properties of these indolone-*N*-oxides were controlled by a bioreductive transformation in red blood cells [16].

Many parameters including solubility and log P, absorption, diffusion and metabolism, as well as the cellular targets affect the biological activities of compounds. It is clear that a global analysis of each parameter versus the biological activity studied may not produce a clear relationship. The effects of these parameters may be additive or subtractive, rendering any correlation difficult to observe on a large series. No simple relationship was found between the reduction potential and the antiplasmodial activity. For example, one can note that compounds with aliphatic substitutions (**49**, **50** and **60**) are hardly reduced and poorly active against *Plasmodium*. On the contrary, compounds having amine groups (**26**, **30** and **68**) also have very cathodic reduction potentials whereas they are among the most biologically active compounds of the series. The amine groups at R^3 on these compounds give cationic protonated forms at the pH of the cell model tested (parasitized red blood cells), which are determinant for the absorption mechanism of the cell. In the case of these compounds (**26**, **30** and **68**), the absorption surpasses the electron withdrawing effects of substituents compared with other compounds. Interestingly, we

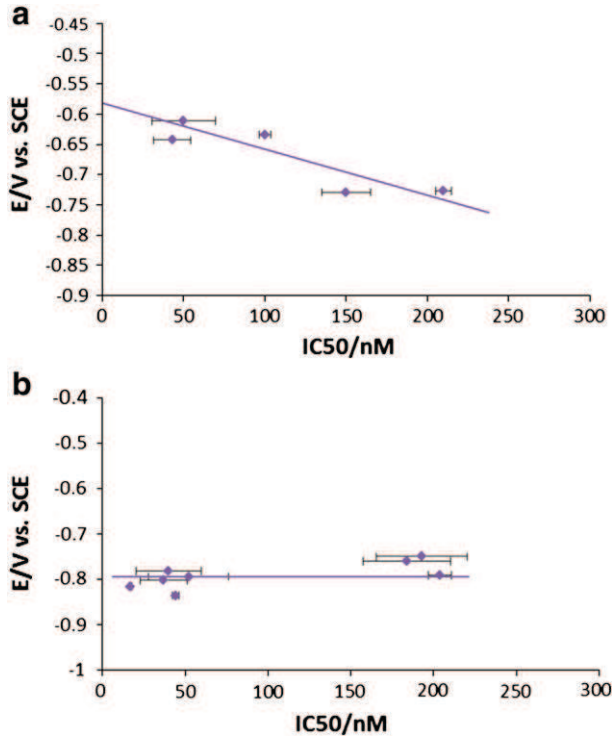

Fig. 5. Relationship between antiplasmodial activity and reduction potential. Plot of $E_{1/2}$ against IC_{50} for a) compounds having the methoxy group (R^1) and electron-withdrawing substituents on the phenyl group at R^3 (**9**, **11**, **12**, **13**, **37**); b) compounds having the methoxy group (R^1) and electron-donating substituents as R^3 (**17**, **18**, **22**, **24**, **27**, **29**, **40**, **42**).

previously showed that antiplasmodial activities were more strongly affected by the substitutions at R^3 than by substitutions at the phenyl group of the indolone moiety (R^1 and R^2). Consequently, the relationship between activity and the ease of reduction have been studied for molecules with $R^1 = —OCH_3$ and $R^2 = H$, compounds distinguished by electron-withdrawing or -donating substituents on the phenyl group at R^3. The corresponding graphs are shown in Fig. 5. In the case of electron-withdrawing substituents (Fig. 5a), the antiplasmodial activity increases when the compounds are more readily reduced. These results are consistent with an antiplasmodial property controlled by a bioreductive transformation in red blood cells [16] and in agreement with mechanisms of action that we recently reported [14].

On the other hand, for electron-donating substituents (Fig. 5b), a large variation in activity is observed, whereas the potential is almost constant due to their weak influence. In this second case, variation in lipophilicity could explain such disparate IC_{50} values. Indeed, in this group, the less potent compounds **20**, **24** and **42** are characterized by the highest partition coefficient (logP > 3), reaching 3.63 for **42**.

4. Conclusion

The thirty seven indolone-*N*-oxides studied in aprotic solvents, showed two reduction steps located around -0.68 ± 0.2 V and -1.45 ± 0.2 V vs. SCE. The first reduction step was reversible for all the compounds studied under the conditions of the study and ascribed to the reduction of the —C=N—O double bond, whereas the second irreversible reduction step was ascribed to the carbonyl reduction. EPR spectroscopy analysis confirmed that this first reduction gives rise to the formation of a relatively stable radical, which could be the starting point for the redox events deleterious to the parasite. A relationship between electrochemical behavior and indolone-*N*-oxide structure can be established for compounds having electron-withdrawing substituents. The insertion of an electron-withdrawing group on the *N*-oxide ring results in a less negative reduction potential making the bio-reduction easier and thus the compound more active against *Plasmodium*. These results will orientate the selection of substituents for the design of new molecules with better pharmacological activities.

Acknowledgements

This work was supported by the European Commission (FP6-LSH-20044-2.3.0-7, STREP no. 018602, Redox antimalarial Drug Discovery, READ-UP), IDEALP'Pharma and The French National Research Agency (ANR-10-BLAN-0726, Mechanisms of action and Targets of new antimalarial Redox molecules, MATURE). We thank J.-P. Nallet and IDEALP'Pharma for their scientific contributions.

References

[1] I. Aldana, M.A. Ortega, A. Jaso, B. Zarranz, P. Oporto, A. Gimenez, A. Monge, E. Deharo, Anti-malarial activity of some 7-chloro-2-quinoxalinecarbonitrile-1,4-di-N-oxide derivatives, Pharmazie 58 (2003) 68–69.
[2] E. Vicente, L.M. Lima, E. Bongard, S. Charnaud, R. Villar, B. Solano, A. Burguete, S. Perz-Silanes, I. Aldana, L. Vivas, A. Monge, Synthesis and structure–activity relationship of 3-phenylquinoxaline 1,4-di-N-oxide derivative as antimalarial agents, Eur. J. Med. Chem. 41 (2008) 1903–1910.
[3] G. Aguirre, H. Cerecetto, R. Di Maio, M. Gonzalez, M.H. Montoya Alfaro, A. Jaso, B. Zarranz, M.A. Ortega, I. Aldana, A. Monge-Vega, Quinoxaline N, N′-dioxide derivatives and related compounds as growth inhibitors of *Trypanosoma cruzi*. Structure–activity relationships, Bioorg. Med. Chem. Lett. 14 (2004) 3835–3839.
[4] E. Moreno, S. Pérez-Silanes, S. Gouravaram, A. Macharam, S. Ancizu, E. Torres, I. Aldana, A. Monge, P.W. Crawford, 1,4-Di-N-oxide quinoxaline-2-xcarboxamide: cyclic voltammetry and relationship between electrochemical behavior, structure and anti-tuberculosis activity, Electrochim. Acta 56 (2011) 3270–3275.
[5] W. Porcal, P. Hernandez, G. Aguirre, L. Boiani, M. Boiani, A. Merlino, A. Ferreira, R. Di Maio, A. Castro, M. Gonzalez, H. Cerecetto, Second generation of 5-ethenylbenzofuran derivatives as inhibitors of *Trypanosoma cruzi* growth : synthesis, biological evaluation and structure–activity relationships, Bioorg. Med. Chem. 15 (2007) 2768–2781.

[6] M. Boiani, L. Piacenza, P. Hernandez, L. Boiani, H. Cerecetto, M. Gonzalez, A. Denicola, Mode of action of Nifurtimox and N-Oxide-containing heterocycles against *Trypanosoma cruzi*: is oxidative stress involved? Biochem. Pharmacol. 79 (2010) 1736–1745.
[7] A. Gerpe, G. Aguirre, L. Boiani, H. Cerecetto, M. González, C. Olea-Azar, C. Rigol, J.D. Maya, A. Morello, O.E. Piro, V.J. Arán, A. Azqueta, A. López de Ceráin, A. Monge, M.A. Rojas, G. Yaluff, Indazole N-oxide derivatives as antiprotozoal agents: synthesis, biological evaluation and mechanism of action studies, Bioorg. Med. Chem. 14 (2006) 3467–3480.
[8] M. Hooper, D.A. Patterson, D.G. Wibberley, Preparation and antibacterial activity of isatogens and related compounds, J. Pharm. Pharmacol. 17 (1965) 734–741.
[9] A.B. Sahasrabudhe, H.V. Kamath, B.V. Bapat, N.K. Sheshgiri, Antitubercular agents: part III-synthesis of substituted 2-arylisatogens, Indian J. Chem. 19 (1980) 230–232.
[10] H. Hagen, R.D. Kohler, E.H. Pommer, Isatogen derivatives and their use as fungicides, Eur. Pat. 54147, Chem. Abstr. 97 (1982) 216185.
[11] H. Cerecetto, M. González, N-oxides as hypoxia selective cytotoxins, Mini Rev. Med. Chem. 1 (2001) 219–231.
[12] F. Nepveu, S. Kim, J. Boyer, O. Chatriant, H. Ibrahim, K. Reybier, M.C. Monje, S. Chevalley, P. Perio, B. Lajoie, E. Deharo, M. Sauvain, R. Tahar, L. Basco, A. Pantaleo, F. Turrini, P. Arese, A. Valentin, E. Thompson, L. Vivas, S. Petit, J.-P. Nallet, Synthesis and antiplasmodial activity of new indolone N-oxide derivatives, J. Med. Chem. 53 (2010) 699–714.
[13] R. Tahar, L. Vivas, L. Basco, E. Thompson, H. Ibrahim, J. Boyer, F. Nepveu, Indolone-N-oxide derivatives: in vitro activity against fresh clinical isolates of *Plasmodium falciparum*, stage specificity and in vitro interactions with established antimalarial drugs, J. Antimicrob. Chemother. 66 (2011) 2566–2572.
[14] A. Pantaleo, E. Ferru, R. Vono, G. Girbaldi, O. Lobina, F. Nepveu, H. Ibrahim, J.-P. Nallet, F. Carta, F. Mannu, P. Pippia, E. Campanella, P.S. Low, F. Turrini, New anti-antimarial indolone-N-oxides, generating stable radical species, promote destabilization of the host cell membrane at early stages of *P. falciparum* growth, Free Radic. Biol. Med. 52 (2012) 527–536.
[15] N. Ibrahim, H. Ibrahim, S. Kim, J.P. Nallet, F. Nepveu, Interactions between antimalarial indolone-N-oxide derivatives and human serum albumin, Biomacromolecules 11 (2010) 3341–3351.
[16] H. Ibrahim, A. Pantaleo, F. Turrini, P. Arese, J.-P. Nallet, F. Nepveu, Pharmacological properties of indolone-N-oxides controlled by a bioreductive transformation in red blood cells, Med. Chem. Commun. 2 (2011) 860–869.
[17] J. Boyer, V. Bernardes-Genisson, V. Farines, J.P. Souchard, F. Nepveu, 2-Substituted-3-H-indol-3-one-1-oxides: preparation and radical trapping properties, Free. Radic. Res. 38 (2004) 459–471.
[18] N.G. Tsierkezos, Investigation of the electrochemical reduction of benzophenone in aprotic solvents using the method of cyclic voltammetry, J. Sol. Chem. 36 (2007) 1301–1310.
[19] N.A. Macias-Ruvalcaba, D.H. Evans, Electrochemical reduction of 2-fluorenecarboxaldehyde: a mechanism with a grandparent–grandchild reaction, J. Electroanal. Chem. 585 (2005) 150–155.
[20] D.C. de Azevedo, J.F.C. Boodts, J.C.M. Cavalcanti, A.E.G. Santana, A.F. dos Santos, E.S. Bento, J. Tonholo, M.O.F. Goulart, Self-protonation mechanism in the electrochemical reduction of Jatropholone, J. Electroanal. Chem. 5466 (1999) 99–106.
[21] P.-L. Fabre, L. Latapie, A. Noirot, N. Chouini-Lalanne, Correlation of cyclic voltammetry behaviour and photooxidative properties of indoprofen and its photoproducts, Electrochim. Acta 52 (2006) 102–107.
[22] S. Michaud, V. Hajj, L. Latapie, A. Noirot, V. Sartor, P.-L. Fabre, N. Chouini-Lalanne, Correlations between electrochemical behaviours and DNA photooxidative properties of non stereoïdal anti-inflammatory drugs and their photoproducts, J. Photobiol. Photochem. B, 110 (2012) 34–42, http://dx.doi.org/10.1016/j.jphotobiol.2012.02.007.
[23] J.M. Savéant, D. Tessier, Potential dependence of the electrochemical transfer coefficient. Reduction of some nitro compounds in aprotic media, J. Phys. Chem. 81 (1977) 2192–2197.
[24] M. Aravena, R. Figueroa, C. Olea-Azar, V.J. Aran, Esr Electrochemical and orac studies of nitro compounds with potential antiprotozoal activity, J. Chil. Chem. Soc. 55 (2010) 244–249.
[25] D.B. Adams, M. Hooper, J.S. Christopher, S.E. Raper, B. Stoddart, Isatogens: crystal structure, electron density calculations, and 13C nuclear magnetic resonance spectra, J. Chem. Soc. Perkin 1 (6) (1986) 1005–1010.
[26] C.C. Bond, M. Hooper, Isatogens. Part VI. Synthesis of isatogens via tolan (diphenylacetylene) intermediates, J. Chem. Soc. C (1969) 2453–2460.
[27] J.E. Bunney, M. Hooper, Isatogens Part VII. Polarographic reduction of isatogens, J. Chem. Soc. B (1970) 1239–1241.
[28] B. Tuccio, P. Bianco, J.C. Bouteiller, P. Tordo, Electrochemical characterisation of β-phosphorylated nitrone spin traps, Electrochim. Acta 44 (1999) 4631–4634.
[29] G.L. McIntire, H.N. Blount, H.J. Stronks, R.V. Shetty, E.G. Janzen, Spin trapping in electrochemistry. 2. Aqueous and nonaqueous electrochemical characterizations of spin traps, J. Phys. Chem. 84 (1980) 916–921.
[30] P. Zuman, Substituent Effects in Organic Polarography, Plenum Press, New York, 1967.
[31] C. Hansch, A. Léo, R.W. Taft, A survey of Hammett substituent constants and resonance and field parameters, Chem. Rev. 91 (1991) 165–195.